Ductile–brittle transition in Charpy and CT tests / Experiments and modelling

B. TANGUY, J. BESSON, R. PIQUES and A. PINEAU

Centre des Matériaux, ENSMP, BP 87, Evry cedex 91003, France

ABSTRACT: *The objective of this paper is to study Charpy–V notch and CT tests in the ductile–brittle transition range from both an experimental and numerical aspects. Tests were carried out between* $-165°C$ *and* $100°C$ *on Charpy–V specimens using an instrumented pendulum and between* $-60°C$ *and* $0°C$ *on CT30 sidegrooved specimens. Numerical simulations of both tests are presented where ductile damage is simulated by Rousselier model and cleavage fracture using Beremin model. Differences between the stress field ahead of a propagating ductile crack in both specimen geometry are underlined. Calculations are then post–processed to determine the failure probability in the transition temperature range under investigation.*

INTRODUCTION

In spite of its importance in structural integrity assessment, the evaluation of embrittlement of nuclear reactor vessels (RPVs) components has been based on qualitative notch–impact tests for several decades. However toughness values are required to assess the structural integrity. The establishment of a non–empirical, micromechanically based relationship, between the Charpy impact energy and the fracture toughness in the ductile–brittle transition still remains the aim of many researches in the frame of local approaches methodology. This approach is based on the description of the local stress–strain fields and the understanding of the mechanisms involved in fracture. This study is devoted to finite element (FE) modelling of Charpy–V notch and CT specimens in the ductile–brittle transition where two fracture mechanisms are competing : ductile crack growth and transgranular cleavage. Particular attention is paid to the stress–strain fields in front of the crack or notch tip, in particular when stable ductile crack growth has developed. Calculations are then post–processed in order to simulate the ductile–brittle transition

behaviour.

MATERIAL AND TESTING

This study was performed on A508 (16MND5) steel (C= 0.16, Mn= 1.33, S= 0.004, Ni= 0.76, Mo= 0.51 (wt%)) which is used in pressurized water nuclear reactors. The material contains small round MnS inclusions with a volume fraction equal to 1.7510^{-4}. The plastic behavior of this type of material depends both on strain rate and temperature. The material behavior was tested over the temperature range between $-150°\mathrm{C}$ to $200°\mathrm{C}$. Full details about the tests results are given elsewhere [1, 2, 3]. Standardized ISO–V (Charpy–V) specimens according to DIN EN 10045 were tested at temperatures between $-165°\mathrm{C}$ and $+100°\mathrm{C}$ with an instrumented 300J–Pendulum corresponding to an impact velocity of 5.5 ms^{-1}. Elastic–plastic fracture toughness tests with CT30 (thickness 30 mm) 20% side–grooved (3 mm each side with a radius $\rho = 0.25\mathrm{mm}$) specimens were also performed at three specified temperatures, $-60°\mathrm{C}$, $-30°\mathrm{C}$ and $0°\mathrm{C}$. In the ductile–brittle transition range, fracture resistance, J_c, is determined from the J–integral at the initiation of unstable cleavage, $J_c = \eta_0 \frac{U_c}{B_n(W-a_0)}$ (U_c area under the $P-\delta$ curve until cleavage instability, η_0 geometry dependent parameter (ASTM E 813), B_n sidegrooved specimen thickness ($B_n = 24$ mm)). The fracture toughness, K_{Jc}, is then computed as $K_{Jc} = \sqrt{\frac{J_c E}{1-\nu^2}}$ (ASTM E 813). For CT specimens, fully brittle fracture was obtained at $-60°\mathrm{C}$, whereas fully ductile fracturewas observed at $0°\mathrm{C}$. At $-30°\mathrm{C}$, final failure by cleavage occurs after different amount of ductile crack growth.

MODELING

The description of the material behavior, including plastic deformation and ductile damage can be found in [4]. It is based on the Rousselier model [5] modified to account for viscosity, adiabatic heating and damage nucleation.

Brittle fracture was described using the Beremin model [6] which accounts for the random nature of brittle fracture. It can be applied as a post–processor of calculations including ductile tearing. Care must be taken when computing the failure probability of Charpy and CT specimens as ductile crack advance leads to unloading of the material left behind the crack front [4]. Model

parameters were adjusted using round bars tested at low temperatures (-196, $-165^{\circ}\mathrm{C}$) in order to obtain brittle fracture only [4].

SIMULATION OF THE CHARPY–V AND CT TESTS

The finite element meshes used to model both tests are shown in fig. 1. Due to symmetries, only one quarter of the specimen is meshed with the usual boundary conditions. The numerical procedures used to perform the calculations are detailed in [7]. For Charpy–V specimen, a mixed 2D/3D mesh is used to reduce the number of degrees of freedom. The 2D part is computed assuming plane stress (PS) conditions. Contact between the striker, the support and the specimen is also accounted for, using a friction coefficient equal to 0.1. For CT specimen, a 3D mesh with side grooves is used. 2D plane strain (2D DP) simulations were also performed. All results referring to 2D DP simulations assume a specimen thickness of 24 mm ($B = B_{net}$).

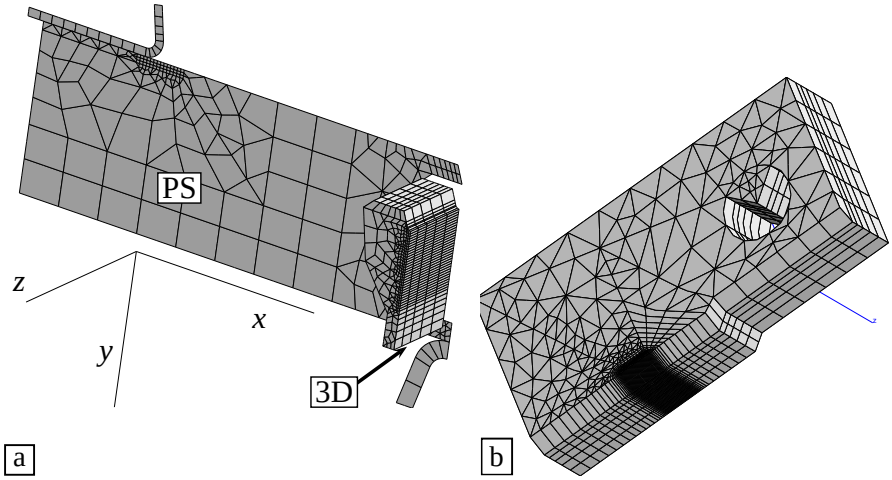

Figure 1: (a) Combined plane–stress (PS) and 3D mesh used for Charpy–V test simulations. (b) 3D mesh used for CT30 test simulations

Stress distribution : 2D plane strain versus 3D simulations

Previous studies (see eg. [4, 8]) have shown that a 3D simulation is necessary for the Charpy test when the deformation of the specimen is important. For CT specimens, it is usually considered that side–grooved specimens could

be modelled with a 2D DP hypothesis, because side–grooves delay the loss of constraint effect, even for large amount of plasticity. Nevertheless in the temperature range where ductile crack growth initiates and propagates, this hypothesis has to be examined. In Fig. 2 computed and experimental force–CMOD (Crack Mouth Opening Displacement) are compared at two different temperatures corresponding to fully brittle fracture ($T = -60°\mathrm{C}$) and transition domain ($T = -30°\mathrm{C}$). At the lower temperature a good agreement is obtained with both modelling. At the higher temperature, 2D DP modelling appears to underestimate the load. Further results are shown in fig. 3 where the maximum principal stress distribution in the center plane of the specimen is plotted for different J_c values. Similar stress distributions are observed up to $J_{c_1} = 185\mathrm{kJ/m^2}$ corresponding approximately to the limit load of the specimen (see fig. 2–b). For higher J_c values, 2D DP hypothesis leads to different stress distribution, due to the earlier ductile crack initiation. Stress profiles can also be compared for an identical ductile crack advance ($\Delta a = 0.5\mathrm{mm}$). 3D computations lead to a slightly higher maximum stress value in the center of the specimen, and also to a larger zone with high stresses. Evolution of failure probability, P_r, versus J_c (fig. 3–b) underlines the differences between 2D DP and 3D computations, 2D DP hypothesis predicting a more brittle behavior.

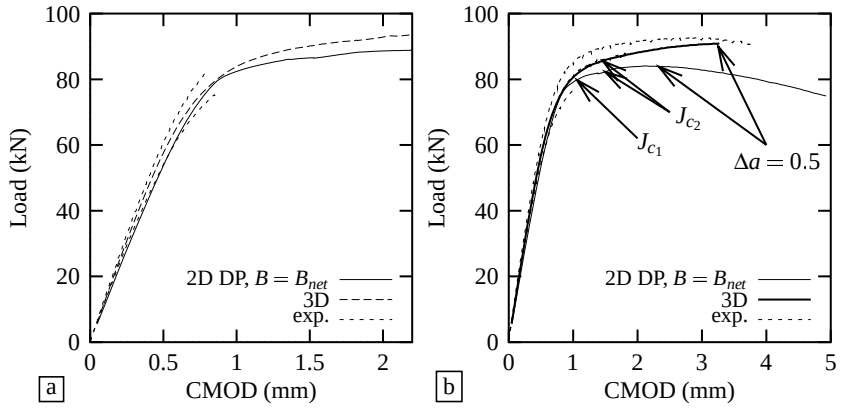

Figure 2: Load–CMOD curves computed with 2D DP and 3D simulations for CT30 specimens and comparison with experiments. (a) $-60°\mathrm{C}$, (b) $-30°\mathrm{C}$.

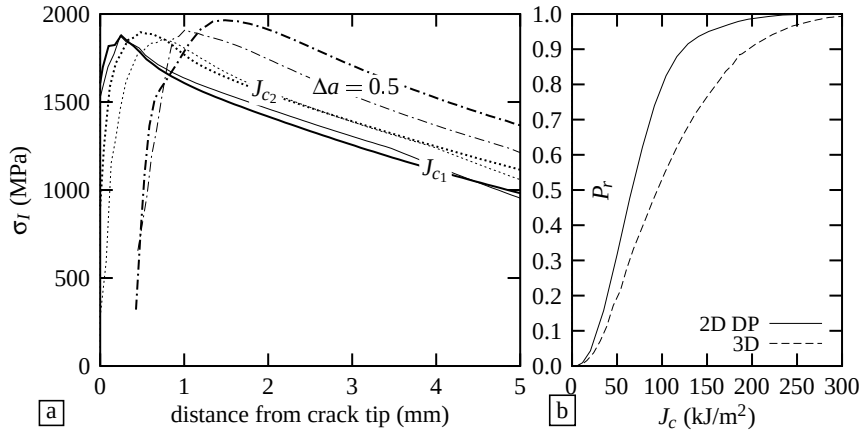

Figure 3: 2D DP (thin lines) versus 3D (thick lines) computations. (a) Maximum principal stress in the mid–section of a CT30 specimen at different J_c values (J_{c_1} =185kJ/m^2, J_{c_2} =307kJ/m^2, $J_c^{3D}(\Delta a = 0.5mm) = 859$kJ/m^2 and $J_c^{2DDP}(\Delta a = 0.5mm) = 550$kJ/m^2). (b) Failure probability, P_r, versus J_c ($T = -30°$C .).

Stress distribution and ductile tearing : CT30 vs Charpy–V specimens

Transgranular cleavage mechanism is often assumed to be described by the Griffith instability criterion, which implies fracture at a critical normal stress near the tip of the crack. The statistical nature of cleavage fracture initiation suggests that the volume of the process zone also plays important role. In the ductile–brittle transition the stresses ahead of the crack are lowered due to the yield stress temperature dependence whereas ductile crack initiates, sampling a greater volume. Ductile tearing initiation and propagation have not the same effects in CT and Charpy–V notch specimens. In the first geometry, ductile crack initiation does not introduce an important increase of the maximum of the principal stress (see curves J_{c_1} and J_{c_2} on fig. 3–a) but an increase of the sampled volume at a given stress. During crack propagation, a slight increase of the stress level is observed (see curves J_{c_2} and $\Delta a = 0.5$mm on fig. 3–a and also fig. 4). Similar results were obtained in a CT25 specimen without side grooves using the Gurson model [9]. In Charpy–V specimen, ductile crack initiation leads to an increase of the stress level (see curves $CVN = 28$J (deflexion, $\delta = 2$mm) and Δa_1 on fig. 4). During crack growth, as in CT

specimen the stress peak is shifted but the maximum stress level continues to increase until a crack length of about 2 mm is reached (see curve Δa_3 and Δa_4 on fig. 4). Afterwards it remains approximately constant. It is also interesting to note that for $T = -30°\mathrm{C}$, the stress peak value is roughly the same in Charpy–V and CT specimens after a ductile crack propagation of approximately 1 mm (CT stress peak value should be slightly higher than that reported in fig. 4 where 2D DP simulation is shown) but the sampled volume is higher in the CT specimen. For further ductile crack propagation the stress peak level is higher in Charpy–V specimen, leading to a lower critical size defect assuming Griffith's criterion. Nevertheless this result has to be confirmed by 3D simulation of large ductile crack propagation in CT specimen.

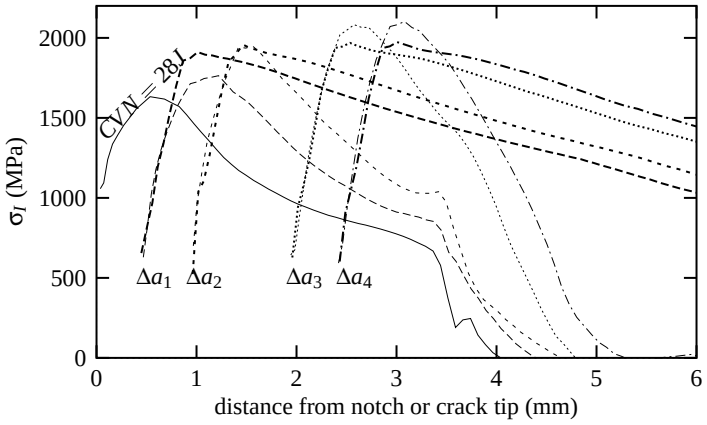

Figure 4: Maximum principal stress in the mid–section of Charpy–V (thin lines) and CT30 (2D DP)(thick lines) specimens during ductile crack growth ($\Delta a_1 = 0.5$mm, $\Delta a_2 = 1$mm, $\Delta a_3 = 2$mm, $\Delta a_4 = 2.5$mm). $T = -30°\mathrm{C}$.

Ductile to brittle transition

The simulations of ductile tearing were post–processed using the Beremin model in order to evaluate the failure probabilities. For each test temperature, the Charpy energy at cleavage instability and fracture toughness values, K_{Jc} corresponding to failure probabilities of 10%, 50% and 90% are shown in fig. 5–a and–b. Using the Weibull parameters determined at low temperature

($m = 17.8$, $\sigma_u = 2925$MPa) leads to a correct evaluation of the Charpy experimental results up to $T = -70°\mathrm{C}$. Engineering parameters like TK_{28} and TK_{68} which are largely used to characterize the transition temperature are well predicted. Above this temperature, the experimental results are underestimated. It is shown that increasing slightly σ_u (by 5% every 30°C starting from $-60°\mathrm{C}$) leads to a good description. Fracture toughness values at cleavage initiation are also underestimated keeping σ_u constant with temperature. A better agreement is obtained when introducing a temperature dependence of σ_u. However this must be confirmed by more K_{Jc} experimental values. This apparent increase in σ_u parameter with temperature was reported by other investigators [9, 10]. It may be related the the effect of large plastic strains on cleavage fracture.

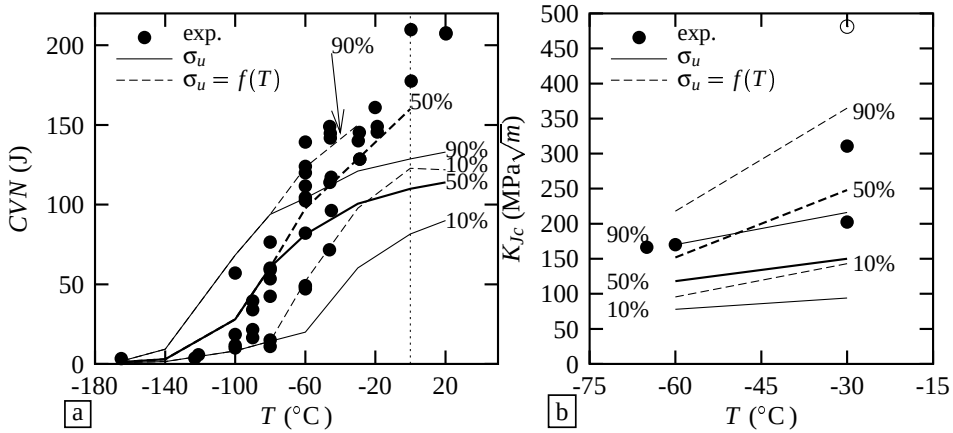

Figure 5: Simulation of the ductile to brittle curve : (a) Charpy–V energy (b) Fracture toughness at cleavage initiation. Dashed lines : transition curve obtained when increasing σ_u by 5% every 30°C starting from $-60°\mathrm{C}$ (open symbol : non-valid test according to ASTM E 813).

SUMMARY

Charpy–V and CT30 specimens were modelled in the ductile–brittle transition regime taking into account the influence of ductile tearing prior to cleavage

failure. Damage models were identified in temperature domains where they act as unique rupture mechanisms. Numerical simulations indicate that a 3D mesh has to be used for the CT specimen in the lower part of the transition regime even if sidegrooved. Ductile tearing strongly modifies the stress field in both specimens : increase of the maximum stress value until a ductile crack length of 2 mm in Charpy specimen, increase of the volume sampled at a given stress with a constant maximum value for CT specimen. The Beremin model is able to describe with a good accuracy the onset of the ductile–to–brittle transition for CVN energies lower than about 80 Joules. Above this value, strain and/or temperature dependence in the Beremin model must be introduced.

REFERENCES

1. Tanguy, B., Piques, R. and Pineau, A. (2001). In: *Proceedings of Charpy Centenary Conference CCC2001*.
2. Tanguy, B., Piques, R., Laiarinandrasana, L. and Pineau, A. (2000). In: *EUROMAT 2000, Advances in Mechanical Behaviour. Plasticity and Damage*, Miannay, D., Costa, P., François, D. and Pineau, A. (Eds.), pp. 499–504. Elsevier.
3. Tanguy, B., Piques, R., Laiarinandrasana, L. and Pineau, A. (2000). In: *ECF 13 , Fracture Mechanics : Applications and Challenges*, Fuentes, M., Elices, M., Martìn-Meizoso, A. and Martìnez-Esnaola, J. (Eds.). Elsevier.
4. Tanguy, B., Besson, J., Piques, R. and Pineau, A. (2001). In: *Proceedings of Charpy Centenary Conference CCC2001*.
5. Rousselier, G. (1987) *Nuclear Engineering and Design*, **105**, 97–111.
6. Beremin, F. (1983) *Met. Trans.*, **14A**, 2277–2287.
7. Besson, J., Steglich, D. and Brocks, W. (2001) *Int. J. Solids Structures*, **38** (46–47), 8259–8284.
8. Schmitt, W., Böhme, W. and Sun, D. (1994). In: *ECF10, Structural Integrity*, pp. 159–170.
9. Hausild, P., Bompard, P., Berdin, C., Prioul, C. and Karlik, M. (2001). In: *Proceedings of Charpy Centenary Conference CCC2001*.
10. Rossoll, A., Berdin, C. and Prioul, C. (2001). In: *Proceedings of Charpy Centenary Conference CCC2001*.